COMPDYN 2013
4th ECCOMAS Thematic Conference on
Computational Methods in Structural Dynamics and Earthquake Engineering
M. Papadrakakis, N.D.Lagaros, V. Plevris (eds.)
Kos Island, Greece, 12–14 June 2013

HIGH-PRECISION FINITE-ELEMENT ANALYSIS OF RUBBER BEARING FOR BASE-ISOLATION OF BUILDING STRUCTURES

Makoto Ohsaki[1*], Tomoshi Miyamura[2], Masayuki Kohiyama[3], Takuzo Yamashita[4], Masashi Yamamoto[5], Naohiro Nakamura[5]

[1]Department of Architecture, Hiroshima University
1-4-1 Kagamiyama, Higashi-Hiroshima 739-8527, Japan
ohsaki@hiroshima-u.ac.jp

[2]Department of Computer Science, College of Engineering, Nihon University
1 Nakagawara, Tokusada, Tamura, Koriyama 963-8642, Japan
miyamura@cs.ce.nihon-u.ac.jp

[3] Department of System Design Engineering, Keio University
3-14-1 Hiyoshi, Kohoku, Yokohama 223-8522, Japan
kohiyama@sd.keio.ac.jp

[4] Hyogo Earthquake Eng. Res. Center, National Res. Inst. for Earth Science and Disaster Prevention
1501-21 Nishikameyama, Mitsuta, Shijimi, Miki 673-0515, Japan
tyamashi@bosai.go.jp

[5]Construction Technology Department, Takenaka Research & Development Institute
1-5-1 Ohtsuka, Inzai 270-1395, Japan
{yamamoto.masashia, nakamura.naohiro}@takenaka.co.jp

Keywords: Rubber Bearing, Finite Element Analysis, Building Frame, Seismic Response, Hyper-Elasticity, Parallel Computing.

Abstract. *Seismic response analysis is carried out for a base-isolated frame. The RC-frame members as well as the rubber bearings are discretized into hexahedral finite elements. The material properties of rubber are represented by the Ogden model, and the frame is assumed to remain in elastic range. The seismic response analysis of the frame, which has more than 3 million degrees of freedom is carried out using the E-Simulator, which is under development at E-Defense, Japan, based on a software package called ADVENTURECluster. It is shown that the global and local responses can be simultaneously evaluated through a high-precision finite element analysis.*

1 INTRODUCTION

Finite element (FE) analysis of laminated rubber bearing is not a well-established field of research. Analysis of rubber material is very difficult because of its incompressibility that leads to constitutive relation using hyper-elastic model. Matsuda *et al*. [1] investigated vertical and lateral stiffnesses of a rubber bearing using FE-analysis. The Mooney-Rivlin model is used for rubber material. Gracia *et al*. [2] developed an overlay model for simulating hyper-elastic and viscoelastic behavior of rubber material. Lejeunes *et al*. [3] presented a numerical reduction model to reduce the computational cost for a thin rubber sheet.

This study is a part of the project called Earthquake Simulator (E-Simulator) at Hyogo Earthquake Engineering Research Center (E-Defense), which belongs to National Research Institute for Earth Science and Disaster Prevention (NIED), Japan. Ohsaki *et al*. [4] demonstrated that seismic responses of an FE-model of a super-highrise steel building frame with more than 70 million DOFs can be evaluated using the E-Simulator, which is based on a parallel FE-analysis software package called ADVENTURECluster (ADVC) [5].

In this study, FE-analysis is carried out for a base-isolated frame utilizing rubber bearing. The rubber sheets and steel plates are discretized into linear hexahedral solid elements. The hyper-elastic constitutive relation is modeled using the Ogden model. It is demonstrated that the experimental results of the laminate rubber bearing under cyclic static deformation can be accurately simulated using the specified material parameters.

The rubber bearings are next attached at the base of a 10-story frame. A horizontal seismic motion is applied to the base-isolated frame, and the interaction between the base and the rubber bearing as well as the detailed local deformation of the isolator is investigated. This way, the details of local and global behavior of the base-isolated building frame can be evaluated simultaneously using a high-precision FE-analysis.

2 RUBBER BEARING MODEL

Consider a rubber bearing model as shown in Fig. 1. The radius of the rubber is 350 mm, and there exists a hole with the radius 7.5 mm at the center. Therefore, the area of rubber is 3.847×10^5 mm^2. The covering rubber on the circumferential surface is neglected.

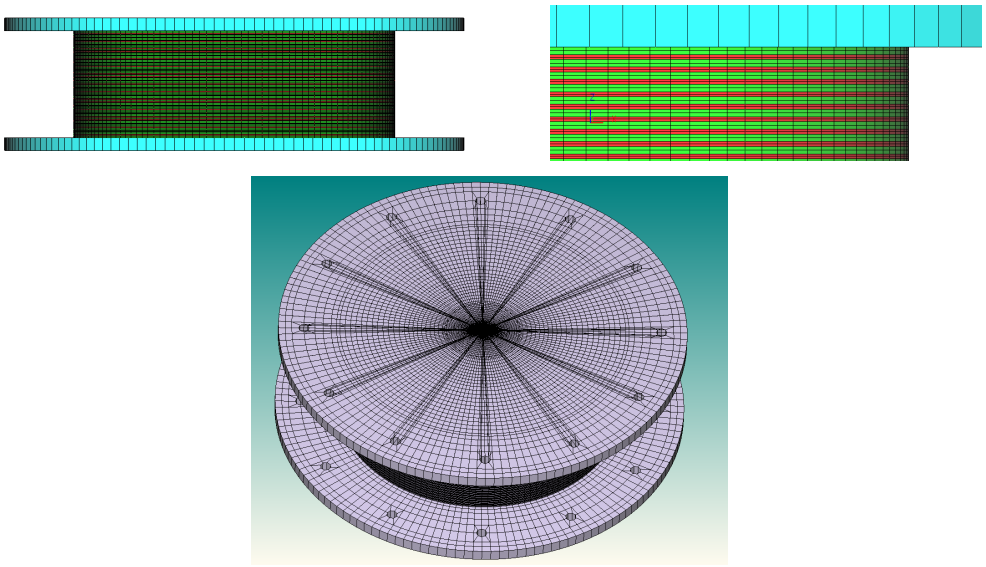

Figure 1: A rubber bearing model.

The rubber bearing has 30 sheets of rubber separated by steel plates. The thicknesses of rubber sheets and steel plates are 4.7 mm and 3.1 mm, respectively. The total height of rubber sheets and steel plates is 230.9 mm. The isolator has top and bottom steel plates called flange with radius 500 mm attached to the rubber/steel plates.

Each rubber sheet is discretized into two layers of hexahedral elements, while each steel plate including flange has only one layer. The numbers of nodes and elements are 502,980 and 486,240, respectively. The number of degrees of freedom is 1,525,002 including the control node defined in Sec. 4.1.

The Ogden model, which is categorized as hyper-elastic material, is used for the natural rubber. The strain energy density function is defined as

$$U = \sum_{n=1}^{2} \frac{\mu_n}{\alpha_n} (\bar{\lambda}_1^{\alpha_n} + \bar{\lambda}_2^{\alpha_n} + \bar{\lambda}_3^{\alpha_n} - 3) + 4.5K(J^{1/3} - 1)^2 \tag{1}$$

where the bulk modulus K is 1000 MPa, and other parameters are $\alpha_1 = 1.6$, $\alpha_2 = 6.2$, $\mu_1 = 0.41$ MPa, and $\mu_2 = 0.0012$ MPa. The variables $\bar{\lambda}_1$, $\bar{\lambda}_2$, $\bar{\lambda}_3$, and J are defined by the left stretch tensor of deformation. The mass density of rubber is 2.00×10^3 kg/m^3. The steel is assumed to be elastic with Young's modulus 205 GPa, Poisson's ration 0.3, and mass density 7.86×10^3 kg/m^3.

A fully integrated linear hexahedral element with eight integration points is used, and geometrical nonlinearity is incorporated using the updated Lagrangian formulation.

3 BASE-ISOLATED FRAME MODEL

Consider a 10-story frame as shown in Fig. 2. The distance between the centers of two rubber bearings is 7000 mm, and the story height is 3500 mm. The upper frame consists of reinforced concrete (RC) columns and beams, which are assumed to remain in elastic range, where Young's modulus is 24 GPa, Poisson's ratio is 0.2, and mass density is 2.3×10^3 kg/m^3. The frame is supported by two rubber bearings that have the same geometry and material properties as Sec. 2.

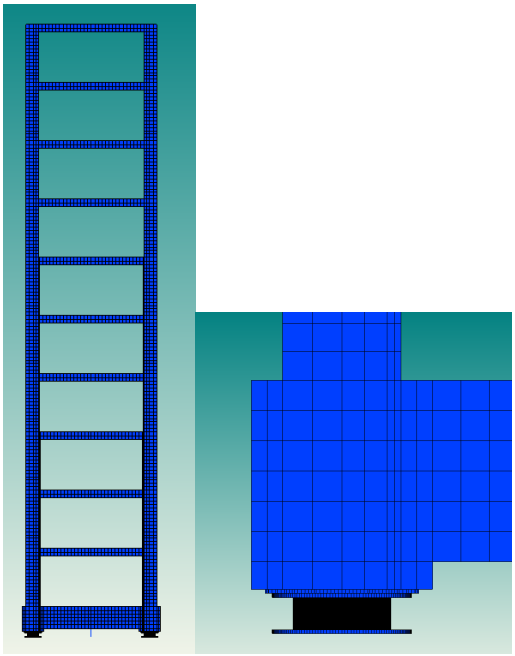

Figure 2: A 10-story base-isolated frame model.

The member sections are listed in Table 1. The height of each footing is 1500 mm. Note that all members have 3-dimensional property although we consider an in-plane deformation. Thus, the out-of-plane displacements of nodes on the plane of symmetry are constrained. The upper surface of flange and the lower surface of footing are connected by contact with sticking condition, i.e., no penetration, gap, or friction is considered.

The weight of RC frame is 1,741 kN, and the total weight including the bases is 1,755 kN. In this case, the mean pressure of the rubber is 2.26 MPa, which is too small. Therefore, considering the loads due to the slab and live loads, the mass density of beams and columns are scaled by the factor 6, which leads to the total weight 10,460 kN and the mean pressure 13.41 MPa.

Table 1: List of member sections.

Column		Beam	
Story	Size	Floor	Size
7 – 10	750×750	7 – Roof	450×750
4 – 6	800×800	4 – 6	450×800
1 – 3	850×850	1 – 3	450×850
		Base	700×1300

4 FINITE ELEMENT ANALYSIS

4.1 Static analysis of rubber bearing

We first carry out cyclic static analysis of single rubber bearing in order to investigate its mechanical properties. The lower surface of the bottom flange is fixed, and the control node is placed at the center of the upper surface of the upper flange. The control node is connected to the nodes on the flange by rigid beams that are represented by multipoint constraints (MPCs), and its rotations along three axes are fixed. The self-weight is first applied, and vertical pressure of 14 MPa is next applied.

Finally, a forced cyclic horizontal displacement is assigned at the control node. The history of displacement (mm) is given as $0 \rightarrow 450 \rightarrow 0 \rightarrow -450 \rightarrow 0$, which is divided into 25 incremental steps in total. The relation between horizontal force and displacement is plotted in solid line in Fig. 3. The curve is close to the experimental result in Ref. [6], which is plotted in dashed lines.

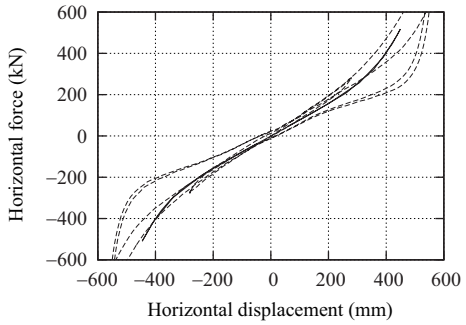

Figure 3: Relation between horizontal force and displacement under pressure of 14 MPa; solid line: numerical result, dashed line: experimental result [6].

The total computational time using 16 cores of Intel Xeon E5-2687W 3.10GHz×2 is 13,487 sec (3.75 hrs); i.e., the average time for single step is 539 sec (8.99 min).

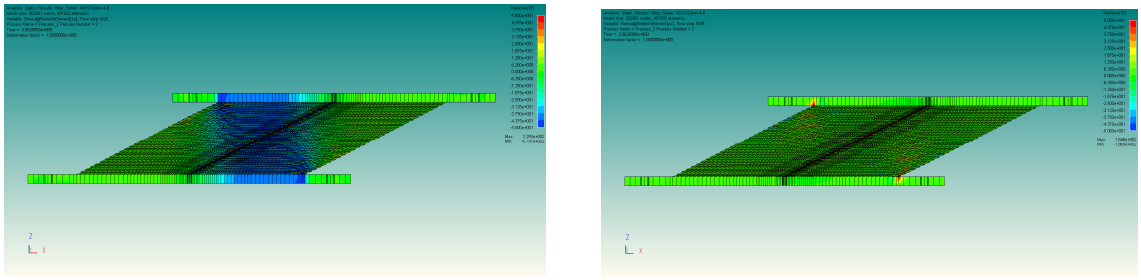

(a) (b)

Figure 4: Stresses at maximum displacement; (a) vertical stress, (b) shear stress.

The vertical and shear stresses at the maximum deformation are shown in Fig. 4 on the section of symmetry. The non-uniform distribution of vertical stress can be clearly seen in Fig. 4(a). By contrast, Fig. 4(b) shows almost uniform distribution of shear stress.

Fig. 5 shows the distribution of normal stress between the upper surface of the top rubber sheet and the lower surface of the upper flange.

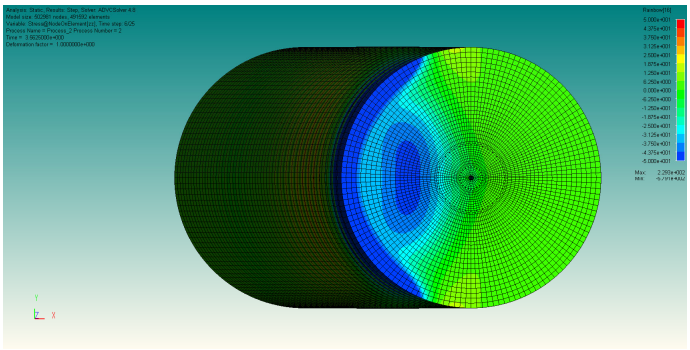

Figure 5: Normal stress between upper flange and rubber.

4.2 Static analysis of base-isolated frame

Horizontal static load, which is proportional to the mass density, is applied incrementally to find horizontal stiffness of the base. The horizontal stiffness obtained by finite difference approximation is plotted in Fig. 6 with respect to the horizontal displacement. As seen from the figure, the stiffness increases, due to material nonlinearity, as displacement is increased.

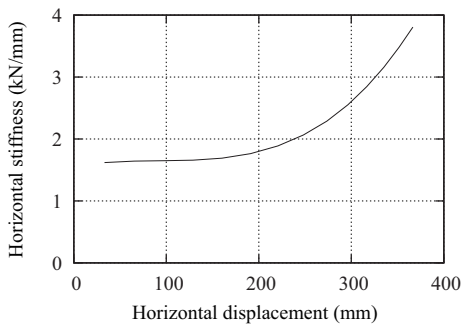

Figure 6: Relation between horizontal displacement and horizontal stiffness of the base.

4.3 Seismic response analysis

A viscous damper is attached between the center of base beam and the ground to incorporate practical situation. If we assume the stiffness 2.5 kN/mm in the displacement range around 300 mm in Fig. 6, and also assume that the upper frame is a rigid body, the first natural period is 4.103 s. Then, the damping coefficient corresponding to the damping factor of 0.15 for the first mode is 489 kN s/mm. The stiffness-proportional damping of 0.03 is given for the upper frame, although the deformation of the upper frame is very small.

The self-weight of the building are first applied. Then, time-history dynamic analysis is carried out to simulate seismic responses of the base-isolated structure. The frame is subjected to the Level-2 design ground motion in Japan, as shown in Fig. 7, which is called BCJ-L2 wave.

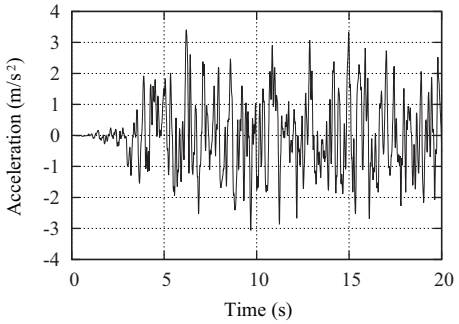

Figure 7: Seismic acceleration (BCJ-L2).

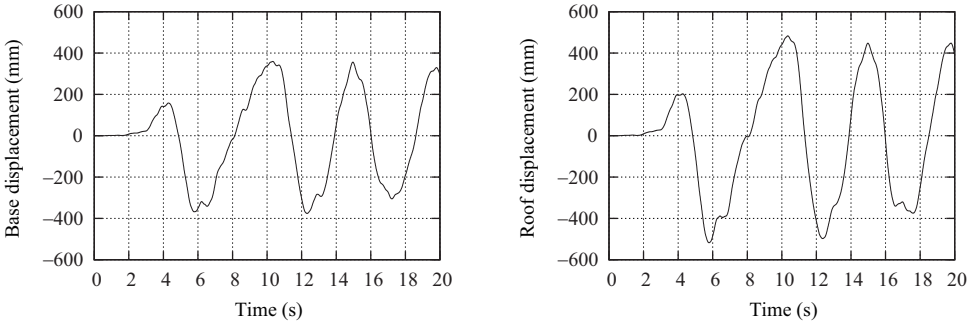

Figure 8: Displacement responses; (a) upper face of rubber bearing, (b) roof.

The total computational time using 16 cores of Intel Xeon E5-2687W 3.10GHz×2 is 1.5811×10^6 sec (18 days and 7.19 hrs) for 2,020 time steps including the initial static analysis for application of gravity; i.e., the average time for single step is 783 sec (about 13.0 min).

Figure 8(a) and (b) show the time histories of relative horizontal displacements at the top of isolator and roof of the frame, respectively. As observed in these figures, the deformation of the frame is very small, and the frame moves as a rigid body with small rocking behavior.

The horizontal and vertical reaction forces are plotted in Fig. 9(a) and (b), respectively. As seen from Fig. 9(b), the vertical reaction force is always positive; i.e., the rubber bearing does not exhibit tensile deformation.

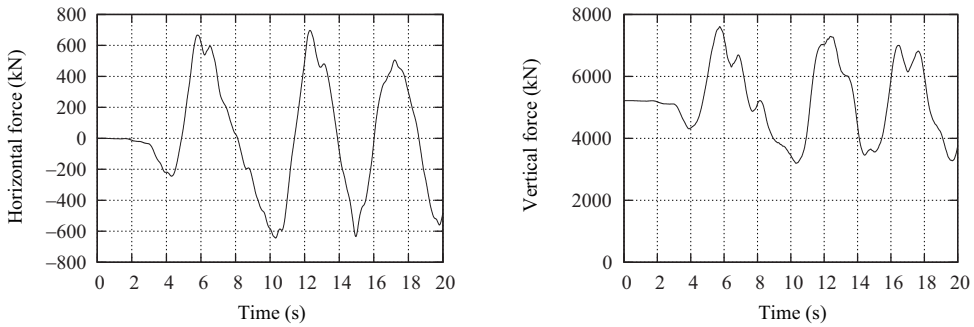

Figure 9: Force responses; (a) horizontal reaction force at fixed supports (base shear force), (b) vertical reaction force at left support.

The maximum and minimum response displacements and reaction forces are listed in Table 2, which confirms that the vertical reaction forces are positive, and the maximum base shear force is about 6.66% of the total weight of the structure. Note that the maximum displacement of the roof relative to the top of the isolator is 149.72 mm, which corresponds to a 0.406%.

Table 2: Maximum dynamic responses

	Disp. of upper-face of isolator	Roof disp.	Horizontal reaction	Vertical reaction (left)	Vertical reaction (right)
Maximum value	359.51	482.95	6.9685×10^5	7.6069×10^6	7.2730×10^6
(Time)	10.33	10.35	12.31	5.74	10.36
Minimum value	−375.84	−517.62	-6.4324×10^5	3.1955×10^6	2.8629×10^6
(Time)	12.28	5.79	10.32	10.31	5.70

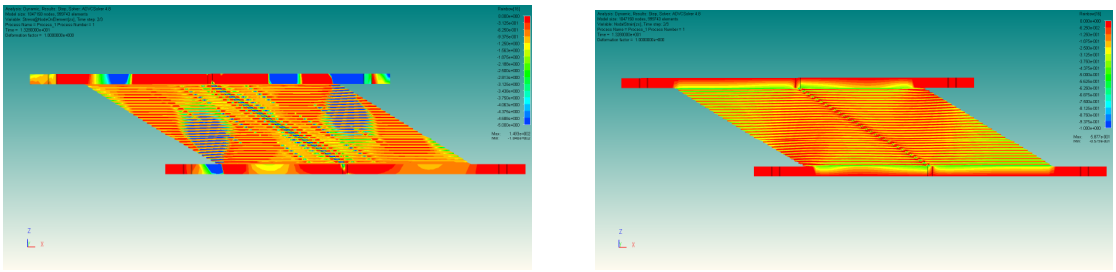

(a) (b)

Figure 10: Shear stress and strain at t = 12.28; (a) stress, (b) strain.

The shear stress and strain are shown in Fig. 10(a) and (b), respectively, at t = 12.28 s, when the absolute value of displacement at the upper-face of isolator becomes maximum. In contrast to the case of static analysis, the shear stress is not uniformly distributed.

The distributions of normal stress due to contact between the upper flange and the rubber at t = 12.28 s and 5.74 s are shown in Fig. 11, respectively. We can confirm that the normal stress is non-uniformly distributed on the surface. The maximum contact stress at t = 12.28 s is 482.6 MPa, which is very large; however, it is located at the edge, and maximum contact stress at nodes next to the edge is 203.2 MPa, which is less than the yield stress of steel. Therefore, a large stress at the edge may be due to coarse mesh division.

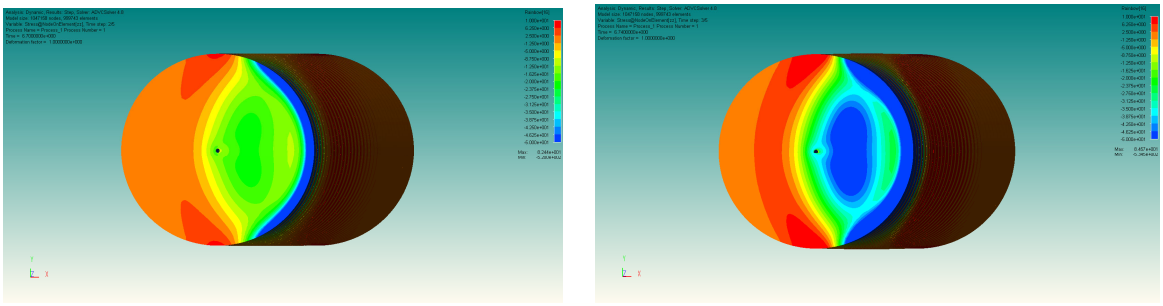

(a) (b)

Figure 11: Normal stress due to contact between upper flange and rubber;
(a) right isolator at t = 12.28 s, (b) left isolator at t = 5.74 s.

5 CONCLUSION

Static and dynamic analyses have been carried out for a 10-story plane frame supported by rubber bearings. It has been demonstrated that the hardening characteristics of the natural rubber are successfully simulated using the Ogden model and fine FE mesh with solid elements.

FE-analysis enables us to investigate simultaneously the global and local responses including the pressure between the layered rubbers and flanges, the distribution of vertical stress in the isolator during cyclic deformation, etc. The computational time for time-history analysis of FE-model with more than 3 million DOFs remains in a practically admissible range using a high-performance PC.

ACKNOWLEDGEMENTS

This study is a part of E-Defense Seismic Experimental Study and Simulation System Development Project conducted by E-Simulator Production Committee (Leader: Prof. Muneo Hori, The University of Tokyo). The authors acknowledge the valuable contribution from the committee members, and the financial support by NIED. The contribution by Dr. Tomonobu Ohyama and Mr. Kiyoshi Yuyama of Allied Engineering Corporation for computation and mesh generation is also acknowledged.

REFERENCES

[1] A. Matsuda, Y. Ohtori, S. Yabana and K. Hirata, Numerical simulation of the loading tests of laminated rubber bearings, *JSME Int. J., Ser. A*, **44**(1), 160-166, 2001.

[2] L. A. Garcia, E. Liarte, J. L. Pelegay and B. Calvo, Finite element simulation of the hysteretic behavior of an industrial rubber. Application to design of rubber components, *Finite Elements in Analysis and Design*, **46**(4), 357-368, 2010.

[3] S. Lejeunes, A. Boukamel and B. Cochelin, Analysis of laminated rubber bearings with a numerical reduction model method, *Arch. Appl. Mech.*, **76**(5-6), 311-326, 2006.

[4] M. Ohsaki, T. Miyamura, M. Kohiyama, M. Hori, H. Noguchi, H. Akiba, K. Kajiwara and T. Ine, High-precision finite element analysis of elastoplastic dynamic responses of super-highrise steel frames, *Earthquake Engineering and Structural Dynamics*, **38**(5), 635-654, 2009.

[5] Allied Engineering Corporation, http://www.alde.co.jp/english/advc/index.html, as of Feb. 13, 2013.

[6] S. Minewaki, M. Yamamoto, M. Higashino, H. Hamaguchi, H. Kyuke, T. Sone, H. Yoneda and A. Wada, Performance tests of full size isolators for super high-rise isolated buildings, *J. Struct. Eng.*, Architectural Inst. Japan, **55B**, 469-477, 2009. (in Japanese)